Langmuir

ARTICLE

pubs.acs.org/Langmuir

Poly(vinyl alcohol) Physical Hydrogels: Noncryogenic Stabilization Allows Nano- and Microscale Materials Design

Bettina E. B. Jensen,[†] Anton A. A. Smith,[†] Betina Fejerskov,[†] Almar Postma,[‡] Philipp Senn,[§] Erik Reimhult,[§,∥] Mateu Pla-Roca,[§] Lucio Isa,[§] Duncan S. Sutherland,[⊥] Brigitte Städler,*[,⊥] and Alexander N. Zelikin*[,†,⊥]

[†]Department of Chemistry, Aarhus University, Denmark

[‡]CSIRO - Materials Science and Engineering, Clayton VIC, Australia

[§]ETH, Zürich, Switzerland

[∥]BOKU - University of Natural Resources and Life Sciences, Vienna, Austria

[⊥]iNANO Interdisciplinary Nanoscience Centre, Aarhus University, Denmark

Supporting Information

ABSTRACT: Physical hydrogels based on poly(vinyl alcohol), PVA, have an excellent safety profile and a successful history of biomedical applications. However, highly inhomogeneous and macroporous internal organization of these hydrogels as well as scant opportunities in bioconjugation with PVA have largely ruled out micro- and nanoscale control and precision in materials design and their use in (nano)biomedicine. To address these shortcomings, herein we report on the assembly of PVA physical hydrogels via "salting-out", a noncryogenic method. To facilitate sample visualization and analysis, we employ surface-adhered structured hydrogels created via microtransfer molding. The developed approach allows us to assemble physical hydrogels with dimensions across the length scales, from ∼100 nm to hundreds of micrometers and centimeter sized structures. We determine the effect of the PVA molecular weight, concentration, and "salting out" times on the hydrogel properties, i.e., stability in PBS, swelling, and Young's modulus using exemplary microstructures. We further report on RAFT-synthesized PVA and the functionalization of polymer terminal groups with RITC, a model fluorescent low molecular weight cargo. This conjugated PVA-RITC was then loaded into the PVA hydrogels and the cargo concentration was successfully varied across at least 3 orders of magnitude. The reported design of PVA physical hydrogels delivers methods of production of functionalized hydrogel materials toward diverse applications, specifically surface mediated drug delivery.

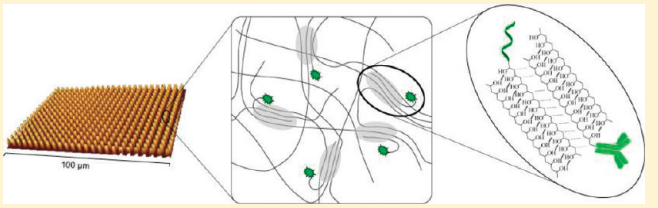

INTRODUCTION

Poly(vinyl alcohol) (PVA) is a polymer with a simple chemical structure, a diversity of peculiar characteristics, and an excellent history of biomedical applications,[1,2] specifically in the form of hydrogel materials and utility in enzyme immobilization,[3] cell encapsulation,[4] clinical applications as embolic bodies,[5] etc. Stabilization of three-dimensional PVA networks can be achieved using chemical[6] (e.g., glutaraldehyde, GA) and physical[1] (e.g., freeze-thawing) treatments, and either technique allows fine-tuning material properties toward desired mechanical characteristics of the matrix for tissue engineering, solute diffusion kinetics for controlled drug delivery, low fouling behavior for controlled tissue compatibility, etc. However, while this research and development goes back for several decades, neither the polymer nor the hydrogels currently appear in the focus of biomedical research. For polymer therapeutics, hydroxyl groups are significantly disadvantaged as compared to "classic" conjugation sites, e.g., amine and thiol functionalities, and the saponification step in the polymer production rules out the use of activated comonomers (e.g., NHS-esters). As a result, reports on PVA used in bioconjugation are solitary. In materials design, GA-stabilization of hydrogels results in potential cytotoxicity of materials[7] as well as a loss of activity of immobilized proteins. PVA physical gels are benign and therefore more attractive for biomedicine, yet their inhomogeneous interior, high porosity,[1,2] and structural defects sized up to hundreds of micrometers[8] largely rule out micro- and nanoscale materials design as well as controlled loading, retention, and release of cargo. Due to this, in their current form, PVA hydrogels failed to meet the demands of (nano)biotechnology and were lost from the mainstream of biomedical research. Nevertheless, an excellent safety profile and FDA approval for diverse uses[9] make reconsideration of PVA based materials from a different point of view highly promising.

Herein, we describe the first example of nano- and microscale control over PVA physical hydrogels, develop structurally stable physical hydrogels with dimensions ranging from macroscopic

Received: April 29, 2011
Revised: June 16, 2011
Published: July 05, 2011

samples down to ~100 nm, and achieve a loading of model low molecular weight cargo with concentration of the latter varied over several orders of magnitude. To facilitate visualization and characterization of hydrogels, we chose to investigate surface-adhered materials and used microtransfer molding (μTM) as a main tool to create micro- and nanostructured hydrogels. Using this tool, we investigate a "salting out" procedure (i.e., phase separation induced by addition of low molecular weight electrolytes) to obtain PVA hydrogels and assess the influence of polymer molecular weight and concentration as well as "salting out" time on the properties of the hydrogels, i.e., stability in PBS, swelling, and Young's modulus. Further, we introduce a novel loading concept for a model low molecular weight cargo based on the synthesis of amine-terminated PVA via reversible addition−fragmentation chain transfer polymerization (RAFT) technique, followed by conjugation of model cargo through the terminal amine group and a cogelation of the conjugate with the PVA matrix polymer. We demonstrate that the use of modern tools of polymer chemistry and innovative techniques in materials design afford significantly increased degree of control over the structure and properties of PVA physical hydrogels. We believe that the achieved advances in the nano- and microfabrication using PVA endow these materials with a renewed promise for diverse applications in biotechnology and biomedicine.

EXPERIMENTAL SECTION

Unless stated otherwise, all chemical were obtained from Sigma-Aldrich and used without purification. Commercial PVA with three different MW were used for all the experiments: 13−23 kDa, herein termed low molecular weight, LMW; 89−98 kDa, termed medium molecular weight, MMW; and 146−186 kDa, termed high molecular weight, HMW. All the water used was ultrapure water (Milli-Q gradient A 10 system, resistance 18 MΩ cm, TOC < 4 ppb, Millipore Corporation, U.S.A.). Differential interference contrast (DIC) and fluorescence images were obtained using a Zeiss Axio Observer Z1 microscope.

Synthesis and Fluorescence Labeling of PVA. Prior to polymerization, vinyl acetate (VAc) was purified via distillation, and the initiator 2,2′-Azobis(2-methylpropionitrile) (AIBN) was recrystallized from chloroform. The RAFT agent *O*-ethyl *S*-(phthalimidylmethyl) xanthate was synthesized according to a literature procedure.[10] For polymerization, the RAFT agent (540 mg, 8.83 mmol) and AIBN (20 mg, 0.12 mmol) were dissolved in VAc (18.7 g, 20.0 mL, 0.217 mol). The solution was degassed by four freeze−pump−thaw cycles. The polymerization was carried out for 16 h at 60 °C followed by the precipitation of the polymer from acetone into pentane. The synthesized polymer had a molecular weight of MN (NMR) 9500 Da, MN (GPC) 9100, and a polydispersity (GPC) of 1.17. For removal of the terminal phthalimide group, a solution of poly(vinyl acetate) (1.050 g, 0.1 mmol) in methanol (5 mL) was mixed with hydrazine hydrate (0.5 mL, 10.0 mmol) and stirred for 30 min at 60 °C. The reaction was quenched with 10% hydrochloric acid and precipitated into water. The water was removed by suction filtration and the polymer was washed thoroughly with water. The removal of the phthalimide group was confirmed by NMR spectroscopy. For saponification, amine terminated polymer was dissolved and stirred in a mixture of methanol (50 mL) and 1 mL of NaOH 40% (aq) overnight. Precipitated PVA was isolated via filtration, washed with methanol and dried in vacuo. The yield of the PVA was 480 mg.

For terminal group conjugation with rhodamine isothiocyanate (RITC), amine terminated PVA (100 mg) was dissolved in 1 mL of 0.1 M carbonate buffer, pH 8.3 and charged with 175 μL of 10 g/L solution of RITC in DMSO. The reaction was incubated overnight after which the polymer was isolated by gel filtration on a PD-10 Sephadex G-25 M column and freeze-dried. The yield of PVA-RITC was 54 mg. In a separate experiment it was verified that under the same reaction conditions a sample of commercial, non amine-terminated PVA afforded a negligible degree of conjugation with RITC.

Stamp Fabrication. The required polydimethylsiloxane (PDMS) stamps (Sylgard 184, Dow Corning) were fabricated by PDMS replica molding of either SU-8 2002 or SU-8 3010 photoresist structures (MicroChem, Newton, MA) patterned (2 and 10 μm thick, respectively) on a silicon wafer. The masters for the nanostructures were fabricated according to a previously published protocol using SALI colloidal lithography yielding a random pattern of holes on a silicon wafer at the used surface coverage.[11] The molds were coated with trichloro(1*H*,1*H*,2*H*,2*H*-perfluorooctyl)silane (97%) prior to use in order to prevent PDMS adhesion to the molds during the replication process. The coating procedure was performed in vapor phase (1 h) after oxygen plasma treatment (1 min) of the molds (Technics Plasma 100-E). The base oil and curing agent were mixed in a ratio of 10:1, degassed, and poured over the patterned silicon wafers. The PDMS was cured for 48 h at room temperature.

Microtransfer Molding (μTM) of PVA. Surface-adherent microstructured (μS) PVA films were obtained via μTM. In a typical experiment, the PVA was dissolved in water first at 90 °C, 300 rpm for 3 h, and then equilibrated at 37 °C, 300 rpm overnight, using a thermo shaker (Eppendorf). Prior to use, the PVA solution was heated at 50 °C for 10 min, and then cooled down to 37 °C. Then, the solution was placed between a glass coverslip and a PDMS stamp, and clamped together at finger-tight pressure for several h, after which the stamp was removed to afford a coverslip-adhered μS PVA film ready for the "salting out" post treatment and the subsequent analysis in PBS. A 0.5 M sodium sulfate (Na_2SO_4) "salting out" solution was used in all the experiments. The nanostructured PVA films were made from 12 wt % MMW PVA, left in the clamps for 24 h, "salted out" for 24 h and incubated in PBS for 30 min prior to imaging. For the force curves, the μS PVA films were made from 12 wt % LMW, MMW or HMW PVA, left in the clamps for 3 h, "salted out" for 24 h and left in PBS for 24 h prior to use to ensure a reproducible and homogeneous film.

AFM Imaging and Force Curves. AFM images were recorded on a Nanowizard II BioAFM (JPK, Germany) with soft contact mode cantilevers (CSC38, no Al, MicroMasch), either in air or in PBS. The samples were imaged first in contact mode in order to record the force curve in the center of a cube. The cantilever was calibrated using the JPK SPM software to determine the sensitivity and the spring constant with the thermal noise method. The Young's modulus was derived from the force curves applying the Hertz model in the JPK SPM software assuming a cone shaped tip with a 20° half-cone angle and a Poisson's ratio of 0.5. The results are based on at least 10 force curves of at least three independent samples.

PVA-RITC Loading and Quantification. μS PVA films were prepared as described above using 14 wt % MMW PVA solutions supplemented with PVA-RITC to final concentrations of 10, 1, 0.1, and 0.01 mg/mL PVA-RITC. To ensure a minimal sample-to-sample variation in the surface area covered with μS PVA films, 9 mm diameter cover glass slides and a PDMS stamp with exceeding dimensions were used. Upon disassembly of the clamps (~24 h), excess (overflow) polymer film was removed from the edges of the cover glass slide. The μS PVA films were placed in a 46 well plate and incubated in 200 μL PBS at 37 °C until complete dissolution of the polymer film. The solution was then transferred to a 96 well OptiPlate and the fluorescence intensity was measured at 37 °C using a plate reader (excitation 560 nm; emission 580 nm). To estimate the concentration of PVA-RITC and to calculate the surface coverage, the calibration curve (Supporting Information, Figure S1) for fluorescent intensity (FI) vs concentration of PVA-RITC was obtained by dissolving 2 μL 10 g/L PVA-RITC in 200 μL PBS. A dilution series was carried out by drawing 100 μL of the initial solution

and diluting with 100 μL PBS, etc. using a 96 well plate. The values were used without correction for possible changes in fluorescence due to the presence of PVA.

RESULTS AND DISCUSSION

Structured Physical PVA Hydrogels. To assemble surface-adhered PVA hydrogels, we capitalize on successes of μTM,[12−16] a technique which allows replicating surface characteristics with nano- and microscale precision. The desired surface topography was first replicated from a photoresist structured silicon wafer using PDMS and the resulting microstructured (μS) stamps were further employed in the production of μS PVA hydrogels (Figure 1). To achieve this, PVA solutions were cast between a PDMS stamp and a glass coverslip and incubated in clamps at finger tight pressure. This facile procedure gave rise to coverslip adhered μS PVA thin films, possibly due to a partial dehydration and gelling of PVA. However, the obtained films immediately dissolved upon contact with (buffered) aqueous solutions, and to preserve their shape a post-treatment was required. Our initial experiments revealed that the conventional, cryogenic route of PVA gelation[1,17] was unpractical and offered only a narrow set of conditions to produce μS films stable in physiological conditions. This led us to investigate other means to effect gelation of PVA, and this was accomplished by a "salting out" treatment, i.e., the incubation in a (buffered) solution of a potent kosmotropic salt, sodium sulfate (Na_2SO_4). While a treatment with KOH/Na_2SO_4 mixtures has been previously shown to enhance the mechanical properties of PVA cryogels,[18] to the best of our knowledge, this is the first report on production of noncryogenic PVA hydrogels achieved though Na_2SO_4-induced "salting out" of PVA. With this treatment, we were able to obtain μS PVA hydrogels which remained stable for storage and applications in PBS, Figure 2. PVA physical gels stabilized through a "salting out" treatment appear uniform and retain their structural integrity in a wide range of sizes across the length scales, from nano- (Figure 2A, 80 nm holes; Figure 2B, 500 nm holes) and low micrometer range (Figure 2C, 1 μm sized cubes) to larger, tens and hundred micrometer-sized features, line structures of different widths (Figure 2D-F) and cubic and circular pillars (Figure 2G-I). We note that while the focus of the subsequent presentation lies on characterizing the physical PVA hydrogels, the above-presented surface patterning exerts no limitation on the use of chemical stabilization of PVA hydrogels, which will further broaden the scope and utility of the described technique. We further note that patterning and surface engineering using hydrogels is a powerful approach to guide localization of cells on the surfaces, i.e., cell patterning[19−24] and this has been accomplished using a number of candidate polymers, typically using ∼100 μm topography features and covalent stabilization of the polymer networks. However, topography design and surface engineering using hydrogels with (sub)micrometer precision remains a significant challenge and only a few successful examples were reported.[22,25−27] Furthermore, to the best of our knowledge, there are no prior examples of nano- and micropatterning using physical hydrogels, making our reported results interesting from a fundamental point of view while holding promise to find applications in biomedical

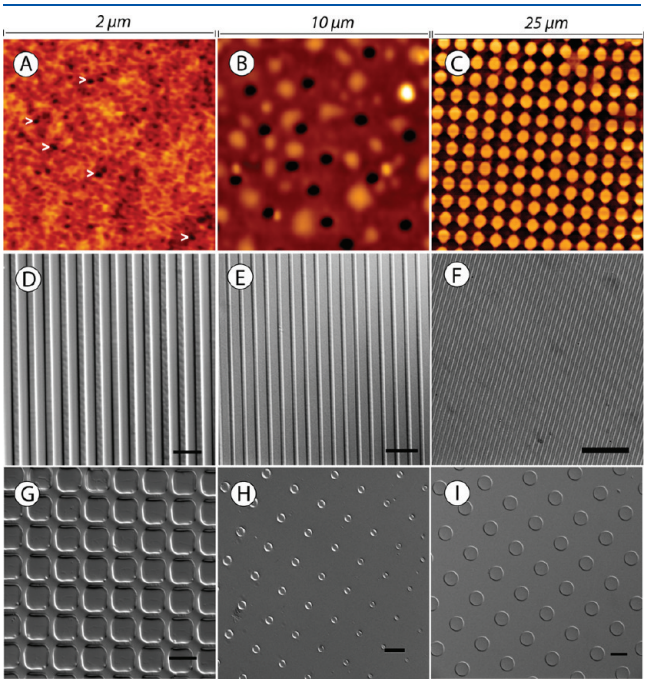

Figure 2. AFM (A−C) and DIC (D−I) images of structured PVA films with varied topography prepared using 12 wt % MMW polymer sample and a 24 h "salting out" treatment, and visualized after a 30 min incubation in PBS. A and B: random ∼80 nm (marked by arrows) and ∼500 nm holes created via μTM using a master made via colloidal lithography. C: 1 μm cubes, scale bars in DIC images are 20 μm (D−G) and 50 μm (H and I).

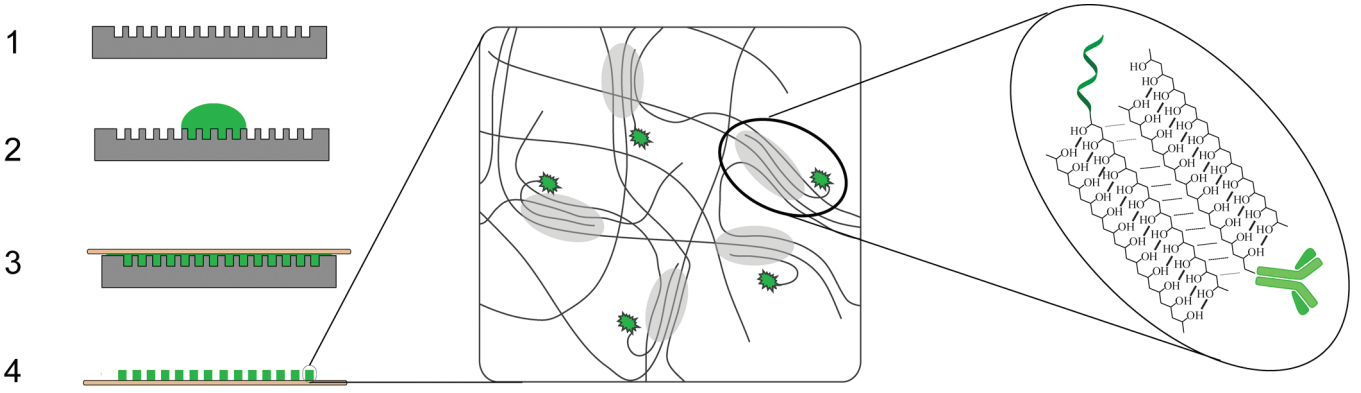

Figure 1. Schematic illustration of microtransfer molding technique employed herein to produce microstructured PVA hydrogels (left) and illustration of internal organization and structure of PVA hydrogels on a macromolecular (right) and supramolecular (middle) levels.

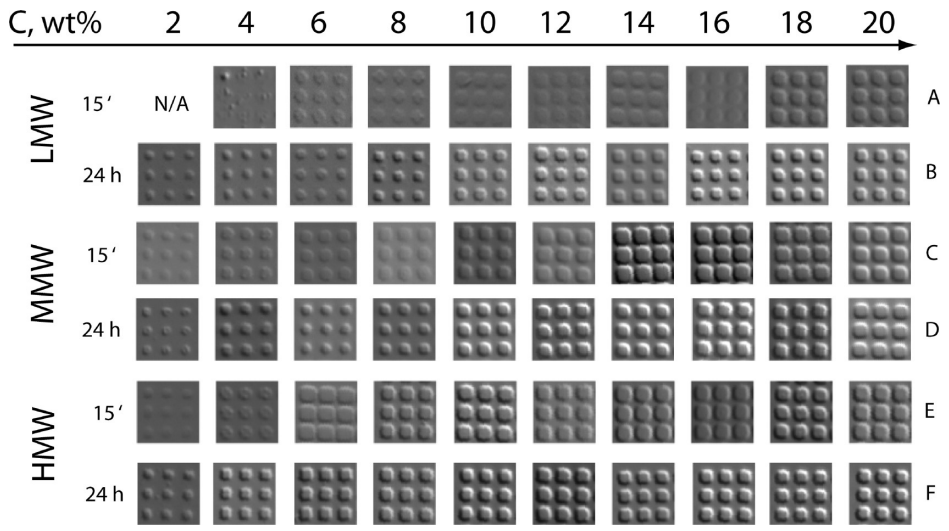

Figure 3. DIC images of μS PVA hydrogels obtained using a PDMS stamp with 2 μm cubic cavities and LMW, MMW, and HMW PVA samples with concentrations from 2 to 20 wt %. For each sample, μS films were subjected to a 15 min (lanes A, C, E) or 24 h (lanes B, D, F) "salting out" treatment, followed by the incubation in PBS for 24 h and imaged in a hydrated state in PBS.

science, i.e., in controlling and guiding cell-surface interactions for cell sheet engineering and/or surface mediated drug delivery.

Stability and Swelling of μS PVA Hydrogels in PBS. Diverse characteristics of PVA physical gels (e.g., Young's modulus, solute diffusion) and even the opportunity to obtain the cryogels as such[28] are dependent on the polymer macromolecular characteristics and concentration, where increasing molecular weight and polymer content are favoring polymer gelation. To investigate this in detail for PVA hydrogels obtained via a "salting out" procedure, we ascertained the range of PVA molecular weights and concentrations which afford micrometer-sized PVA hydrogels stable in PBS through the above-described procedure. To this end, we fabricated 2 μm cubic pillars as an exemplary μS PVA film and used DIC microscopy, a combination which allowed a facile, fast screening of assembly conditions and visualization of the obtained results (Figure 3). Solutions of commercially available LMW, MMW, and HMW PVA and a concentration range from 2 to 20 wt % were employed to produce μS PVA films which were subsequently immersed in a 0.5 M Na_2SO_4 solution for 15 min (Figure 3, lanes A, C, E) or 24 h (Figure 3, lanes B, D, F). Resulting films were further incubated in PBS for 24 h and visualized in a hydrated state, i.e. in PBS without drying. The first remarkable observation from this set of experiments is that upon a 24 h "salting out" treatment (lanes B, D, F) and regardless of polymer concentration and molecular weight, all employed PVA solutions afforded stable surface adhered μS PVA films. In other words, the presented data demonstrate that this novel technique toward stabilization of PVA physical hydrogels can be successfully employed with the use of polymer solutions with concentration as low as 2 wt % and polymer molecular weight as low as 13−23 kDa. This observation comes in stark contrast with PVA cryogels[28] and implies that "salting out" PVA gelation is a more flexible technique as compared to freeze-thawing. Figure 3 also provides for several qualitative observations. With shorter "salting out" time, for each of the three molecular weights there exists an arbitrary lowest concentration required to afford μS PVA films, and this concentration increases with decreasing molecular weight of PVA (~6 wt % for HMW, ~14 wt % for MMW, >20 wt % for LMW). The latter observation is in agreement with a well-documented notion that increased molecular weight of PVA favors polymer gelation.[1] This data set also qualitatively demonstrates that increasing the duration of the "salting out" treatment affords more robust hydrogels (cf. lanes A and B; C and D; E and F), and for each polymer molecular weight and concentration tested, increasing the length of salting out from 15 min to 24 h affords better defined topographic features. An increase in "salting out" time is accompanied by a pronounced shrinkage of the topography features, an effect which is favored by decreased polymer concentration. Also, the data suggest that at a given concentration and "salting out" treatment, LMW hydrogel films appear to exhibit a greater degree of shrinking compared to the films assembled using MMW and HMW samples. Taken together, the employed screening identified several polymer characteristics and solution properties important in the assembly of μS PVA hydrogels and provided an initial investigation into parameters and tools affecting their stability. The presented data demonstrate that μS PVA films can be assembled using a wide range of polymer molecular weights and concentrations.

To gain a further insight into the properties of μS PVA hydrogels, the assembled samples were visualized by AFM. An exemplary film assembled from 10 wt % MMW PVA in air, after "salting out" in Na_2SO_4 solution for 15 min or 24 h and immersed in PBS is shown in Figure 4A. In dry state, there is a dent on top of the features, while swelling of the features in PBS was observed. Images recorded for the samples prepared using 8 wt % LMW, 10 wt % MMW, and 16 wt % HMW PVA were further analyzed to ascertain the dimensions of the topography features in PBS depending on the "salting out" time (Figure 4B). The chosen MWs and concentrations were aiming to illustrate the broad range of starting solutions which accommodated PVA gelation via a "salting out" treatment. A ring-shaped morphology of the topographic features observed for the as-assembled hydrogel films (Figure 4A, left) suggests that during incubation within the PDMS microcavities, the PVA solutions undergo an initial dehydration and possibly an associated accumulation of the polymer at the solution-PDMS interface. AFM analysis further revealed a drastic difference in the swelling behavior for the microstructures assembled using polymer samples differed in

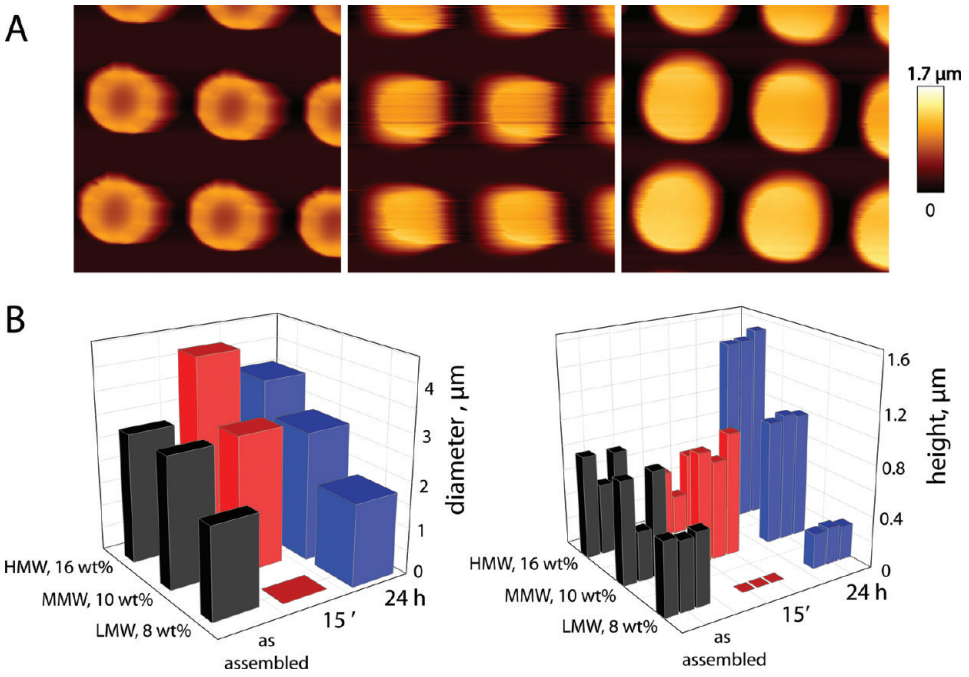

Figure 4. (A) AFM height images of μS PVA films obtained using PDMS stamps with square shaped cavities ($2 \times 2\ \mu m^2$) and a 10 wt % solution of MMW PVA. Images are $10 \times 10\ \mu m^2$ and were obtained in air without post-treatment (left), after a 15 min or 24 h "salting out" and incubation in PBS for 30 min (middle and right, respectively). (B) Topography features diameters and heights (left and right, respectively) for μS surfaces obtained using polymer samples 8 wt % LMW, 10 wt % MMW, or 16 wt % HMW and imaged in air without post-treatment and in PBS after a 15 min or 24 h "salting out" treatment. Height values were taken at the edges (left and right bars in the triplet bars, right graph) and in the center (middle bars in the triplet bars, right graph) of each cube, which combined illustrate the shape of the topography feature.

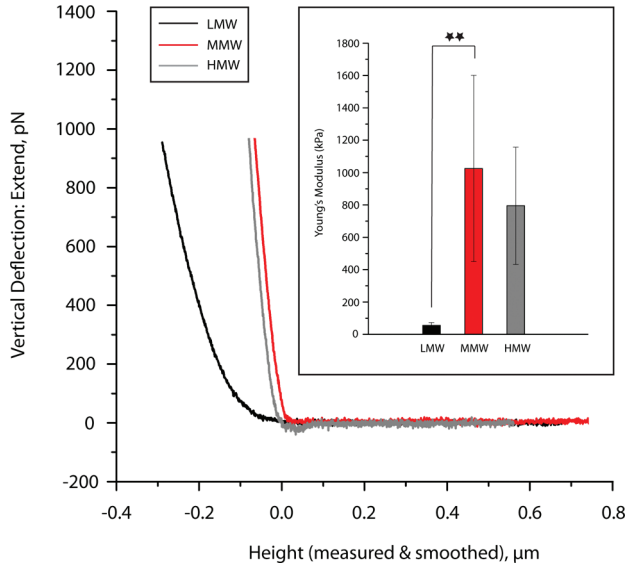

Figure 5. AFM force curve measurements and thereof derived Young's moduli (inset) obtained using μS PVA hydrogels prepared from 12 wt % solutions of LMW, MMW, and HMW PVA. The samples were subjected to a 24 h "salting out" treatment, subsequently incubated in PBS for 24 h and the force curves were collected in a hydrated state in PBS. (**$p < 0.005$).

their molecular weight and concentration. A sample of PVA with the lowest molecular weight and concentration exhibited a pronounced shrinking, particularly in height (Figure 4B, right), a sample of MMW PVA exhibited a minimal change in dimensions upon rehydration, and a sample of HMW PVA with the highest concentration exhibited a pronounced swelling. These observations are qualitatively supported by the data in Figure 3. Interestingly, results in Figure 4 also demonstrate that while as-assembled films from MMW and HMW samples have a pronounced dip in the center, for 8 wt % LMW sample of PVA the polymer redistribution was far less pronounced. This may indicate a differed morphology of the topographic features depending on the molecular weight (and possibly concentration), e.g., core−shell vs a homogeneous hydrogel material, which might be of considerable relevance in the context of drug retention and release properties of the gel.

Mechanical Properties. To investigate the mechanical properties of these hydrogels, we employed force−distance measurements. 12 wt % PVA solutions with varied molecular weights were used to obtain μS hydrogels using a 2 μm cubic stamp, as described above. 12 wt % was chosen because this concentration yielded stable structured film for all molecular weights (Figure 3), making the investigation of the mechanical properties particularly relevant. The assembled films were "salted out" for 24 h and hydrated for 24 h in PBS, after which time the films were subjected to force curve measurements in a hydrated state in PBS (Figure 5). The main conclusion from these experiments is that the Young's modulus for μS hydrogels prepared under the same conditions and differed only in the molecular weight of PVA (LMW vs MMW and HMW) varied by as much as a factor of 10. To verify reproducibility, at least 3 independent samples of μS films were assembled using freshly and independently prepared polymer solutions, and the observed difference in elastic moduli was found to be statistically significant ($p < 0.005$). Presented results also indicate that LMW sample of PVA yielded topography features with a markedly lower value of Young's modulus

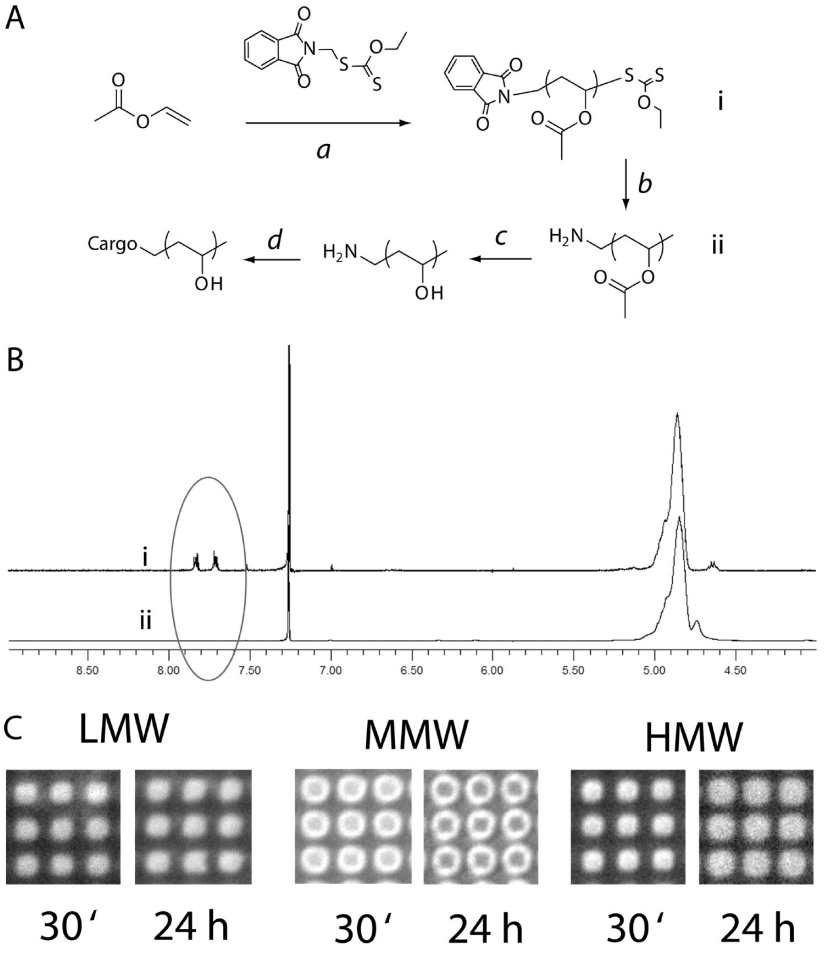

Figure 6. The developed strategy for incorporation of low molecular weight cargo into μS PVA involves conjugation of the cargo to PVA and using the latter as both, a gel forming polymer and an anchor for cargo retention. (A) Illustration of the pathway employed herein for RAFT synthesis of PVA, removal of the terminal phthalimide group and conjugation to a model cargo. (a) RAFT polymerization, (b) hydrozinolysis, (c) saponification, and (d) conjugation. For reaction conditions, see Experimental Section. (B) NMR spectra of polymers before (i) and after (ii) removal of the phthalimide group. The success of this reaction was supported by a disappearance of the NMR signals of phthalimide (circled on the spectra). (C) Fluorescence microscopy images of μS PVA films obtained using a PDMS stamp with 2 μm cubic cavities and 12 wt % PVA solutions with differed MW supplemented with PVA-RITC to 1 g/L. The μS PVA films were subjected to a 24 h "salting out" step, incubated in PBS for 30 min or 24 h and imaged in a hydrated state in PBS.

compared to the MMW or HMW counterparts. This observation is surprising in that LMW features exhibit shrinking (cf. images in Figure 3 and 4) and are therefore smaller and softer at the same time. A plausible explanation relates to a different morphology of topographic features attained for LMW sample as compared to the films obtained using MMW and HMW polymer, as proposed above. It is important to note that numerical values of Young's moduli established above for μS PVA hydrogels are well within the range of elasticity of human tissues,[29] and more importantly, also cover the range of elastic moduli within which adhesion and proliferation of mammalian cells is under an efficient control of matrix mechanics.[30] These results make μS PVA thin films highly attractive candidate biomaterials for diverse biomedical applications.

Cargo Loading and Retention. While typical hydrogels and physical PVA based hydrogels in particular exhibit poor drug retention capabilities, we hypothesized that cargo molecules can be conjugated to PVA, in which case the polymer will serve as both a matrix polymer to form hydrogels and an anchor to ensure drug retention. We further envisioned that conjugation through polymer terminal groups would have a diminished interference with polymer gelation as opposed to conjugation to PVA hydroxyl groups. To this end, we exploit advances in RAFT polymerization technique[31] to produce samples of PVA with desired terminal functionalities.[32] Specifically, we employed a phthalimide (Phth) containing RAFT agent and synthesized a Phth-terminated sample of poly(vinyl acetate) (Figure 6A). Removal of the terminal Phth group using hydrazine was followed by NMR which confirmed a quantitative reaction (Figure 6B), and subsequent saponification using methanolic NaOH yielded an amine-functionalized sample of PVA. Amine functionality is a classic site for bioconjugation and, in contrast with PVA hydroxyl groups, is amenable to facile chemical modification. For proof of concept, the synthesized polymer was used to obtain a conjugate with a model low molecular weight cargo, RITC, the fluorescent nature of which allowed facile visualization of this conjugate incorporated into the hydrogel. Low molecular weight molecules typically have an almost unhindered diffusion through hydrogels and retention of RITC as a PVA-RITC conjugate serves as a thorough test for the proposed method of drug loading.

Three samples of PVA of different MW were prepared at 12 wt % concentration, mixed with PVA-RITC to a 1 g/L concentration

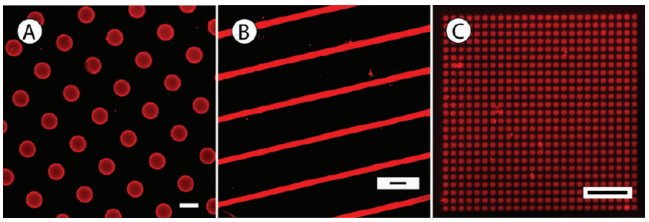

Figure 7. Fluorescence microscopy images illustrating successful PVA-RITC loading into μS PVA films with structures across the length scales, from centimeter long to tens of micrometers and low micrometer sized features. Scale bars: 50 μm (A and B), 20 μm (C).

of the latter and further used in the assembly of PVA hydrogel films. Upon "salting out" treatment (24 h) and incubation in PBS (30 min or 24 h), the cargo loaded μS PVA films were visualized in hydrated state in PBS using a fluorescence microscope (Figure 6C). The presented images show that all the μS hydrogels demonstrate a good retention of incorporated cargo from 30 min up to at least 24 h incubation in a physiological buffer. In subsequent experiments, PVA-RITC was also incorporated into μS PVA hydrogels with topographic features varied in a wide size range, from those well exceeding dimensions of a typical mammalian cell (Figure 7, A and B) to large areas with individual features in the lower micrometer range (Figure 7C). The imaged sample shown in Figure 7B was previously incubated for over 24 h in cell culture media at 37 °C and demonstrates that incorporated cargo is well retained under these conditions. The data in Figures 6 and 7 together demonstrate that the developed protocols for cargo immobilization allows facile preparation of functionalized PVA physical hydrogels with dimensions varied across the length scales.

For surface mediated drug delivery, immobilization of cargo for controlled presentation to adhering cells has been accomplished using a number of techniques.[33] A particular success in the field is associated with recent developments of layer-by-layer polymer deposition technique, a method which allows incorporation and release of diverse candidate therapeutics, e.g., proteins and plasmid DNA. However, this and other methods of surface functionalization offer limited opportunities in controlling the level of loading of low molecular weight molecules. In contrast, Figure 8 demonstrates that surface adhered μS PVA films and the developed cargo immobilization technique afford a control over cargo loading achieved across at least 3 orders of magnitude of cargo concentration. A dramatically enhanced range of attained concentration of immobilized payload is achieved through cogelation of PVA matrix polymer and PVA-cargo conjugate, i.e., using the same polymer as a gel forming material and as an anchor for cargo immobilization. Despite a single-point of cargo conjugation available for each RAFT-derived PVA chain, the mass of immobilized low molecular weight cargo (RITC) was at least similar to the loading of low molecular weight drugs typically reported for the multilayered polymer coatings.[34−37] We emphasize that in surface mediated drug delivery two scenarios are equally important, controlled drug release into bulk solution (mimicking delivery into the bloodstream or surrounding tissue) and presentation of drugs to the adhering cells.[33] A unique feature of the latter mode of drug delivery is that adhering cells may facilitate degradation of the underlying matrix. A further attractive feature of surface mediated drug delivery is that its effectiveness, at least in some reported cases,[38] far exceeds that achieved using the same vectors administered in their solution form, possibly due to a different uptake

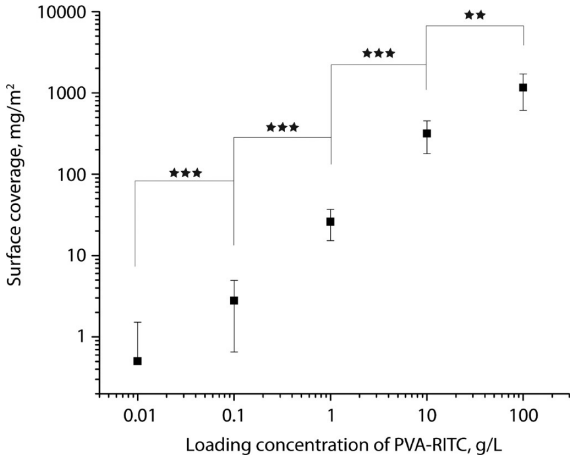

Figure 8. Experimental values of cargo (PVA-RITC) surface coverage obtained with the use of μS PVA hydrogel films and loading solutions with different PVA-RITC concentration. (**$p < 0.01$ and ***$p < 0.001$).

pathway. Our early experiments revealed that cargo retention, as well as kinetics and extent of cargo release from the μS PVA are controlled by several parameters, including macromolecular characteristics of PVA, both matrix forming and used in bioconjugation, and parameters of the "salting out" treatment (data not shown); a detailed presentation on the utility of μS PVA hydrogels in surface mediated drug delivery will be considered in subsequent publications.

CONCLUSIONS

In this work, we assessed fundamental characteristics of PVA physical hydrogels stabilized via a "salting out" treatment. We used μTM and surface adhered hydrogels as convenient tools to monitor success of PVA gelation and visualize the obtained results. We demonstrate the creation of surface adhered PVA hydrogels with dimensions of hydrogel structures varied across the scales, from ~100 nm to centimeters, and their loading with model cargo, the content of the latter controlled over 3 orders of magnitude. We reveal that "salting out" polymer gelation affords stable PVA hydrogels in a wide range of polymer molecular weights and concentrations. The hydrogel properties, i.e., swelling and Young's modulus, were shown to be under an effective control of polymer MW and concentration as well as parameters of the "salting out" treatment. Using the RAFT polymerization technique and a phthalimide RAFT agent, we accomplished the synthesis of PVA samples with terminal amino groups and a facile conjugation to model cargo, RITC. The obtained PVA-RITC conjugates were incorporated into the PVA matrix via simple mixing and cogelation, establishing a flexible platform for controlled cargo loading. We achieved control over topography of microstructured PVA films, mechanical properties of the gels and incorporation of model cargo, all of which combined affords a highly promising platform for biotechnological and biomedical applications, toward controlled cell adhesion and surface mediated drug delivery.

ASSOCIATED CONTENT

Supporting Information. Calibration curve of fluorescent intensity (FI) vs PVA-RITC concentration (g/L). This material is available free of charge via the Internet at http://pubs.acs.org.

AUTHOR INFORMATION

Corresponding Author
*E-mail: bstadler@inano.au.dk (B.S.); zelikin@chem.au.dk (A.N.Z.).

ACKNOWLEDGMENT

This work was supported by grants from the Lundbeck Foundation and Sapere Aude Starting Grants from the Danish Council for Independent Research, Technology and Production Sciences, Denmark (A.N.Z. and B.S).

REFERENCES

(1) Hassan, C. M.; Peppas, N. A. *Adv. Polym. Sci.* **2000**, *153*, 37–65.
(2) Lozinsky, V. I.; Galaev, I. Y.; Plieva, F. M.; Savinal, I. N.; Jungvid, H.; Mattiasson, B. *Trends Biotechnol.* **2003**, *21*, 445–451.
(3) Groger, H.; Capan, E.; Barthuber, A.; Vorlop, K. D. *Org. Lett.* **2001**, *3*, 1969–1972.
(4) Iwata, H.; Totani, T.; Teramura, Y. *Biomaterials* **2008**, *29*, 2878–2883.
(5) Tadavarthy, S. M.; Moller, J. H.; Amplatz, K. *Am. J. Roentgenol.* **1975**, *125*, 609–616.
(6) Bolto, B.; Tran, T.; Hoang, M.; Xie, Z. L. *Prog. Polym. Sci.* **2009**, *34*, 969–981.
(7) Gough, J. E.; Scotchford, C. A.; Downes, S. *J. Biomed. Mater. Res.* **2002**, *61*, 121–130.
(8) Plieva, F. M.; Galaev, I. Y.; Mattiasson, B. *J. Sep. Sci.* **2007**, *30*, 1657–1671.
(9) Nair, B.; panel, C. I. R. E. *Int. J. Toxicol.* **1998**, *17*, 67–92.
(10) Postma, A.; Davis, T. P.; Li, G.; Moad, G.; O'Shea, M. S. *Macromolecules* **2006**, *39*, 5307–5318.
(11) Isa, L.; Kumar, K.; Muller, M.; Grolig, J.; Textor, M.; Reimhult, E. *ACS Nano* **2010**, *4*, 5665–5670.
(12) Zhao, X. M.; Xia, Y. N.; Whitesides, G. M. *Adv. Mater.* **1996**, *8*, 837–840.
(13) Kelly, J. Y.; DeSimone, J. M. *J. Am. Chem. Soc.* **2008**, *130*, 5438–5439.
(14) Buyukserin, F.; Aryal, M.; Gao, J. M.; Hu, W. C. *Small* **2009**, *5*, 1632–1636.
(15) Acharya, G.; Shin, C. S.; McDermott, M.; Mishra, H.; Park, H.; Kwon, I. C.; Park, K. *J. Controlled Release* **2010**, *141*, 314–319.
(16) Merkel, T. J.; Herlihy, K. P.; Nunes, J.; Orgel, R. M.; Rolland, J. P.; DeSimone, J. M. *Langmuir* **2010**, *26*, 13086–13096.
(17) Lozinsky, V. I.; Plieva, F. M. *Enzyme Microb. Technol.* **1998**, *23*, 227–242.
(18) Liu, Y.; Vrana, N. E.; Cahill, P. A.; McGuinness, G. B. *J. Biomed. Mater. Res., Part B* **2009**, *90B*, 492–502.
(19) Liu, V. A.; Bhatia, S. N. *Biomed. Microdevices* **2002**, *4*, 257–266.
(20) Hahn, M. S.; Taite, L. J.; Moon, J. J.; Rowland, M. C.; Ruffino, K. A.; West, J. L. *Biomaterials* **2006**, *27*, 2519–2524.
(21) Seidlits, S. K.; Schmidt, C. E.; Shear, J. B. *Adv. Funct. Mater.* **2010**, *20*, 1368–1368.
(22) Krsko, P.; McCann, T. E.; Thach, T. T.; Laabs, T. L.; Geller, H. M.; Libera, M. R. *Biomaterials* **2009**, *30*, 721–729.
(23) Luo, Y.; Shoichet, M. S. *Nat. Mater.* **2004**, *3*, 249–253.
(24) Suh, K. Y.; Seong, J.; Khademhosseini, A.; Laibinis, P. E.; Langer, R. *Biomaterials* **2004**, *25*, 557–563.
(25) Stiles, P. L. *Nat. Methods* **2010**, *7*, I–Ii.
(26) Diez, M.; Mela, P.; Seshan, V.; Moller, M.; Lensen, M. C. *Small* **2009**, *5*, 2756–2760.
(27) Ahmed, W. W.; Wolfram, T.; Goldyn, A. M.; Bruellhoff, K.; Rioja, B. A.; Moller, M.; Spatz, J. P.; Saif, T. A.; Groll, J.; Kemkemer, R. *Biomaterials* **2010**, *31*, 250–258.
(28) Auriemma, F.; De Rosa, C.; Triolo, R. *Macromolecules* **2006**, *39*, 9429–9434.
(29) Levental, I.; Georges, P. C.; Janmey, P. A. *Soft Matter* **2007**, *3*, 299–306.
(30) Boudou, T.; Crouzier, T.; Nicolas, C.; Ren, K.; Picart, C. *Macromol. Biosci.* **2011**, *11*, 77–89.
(31) Moad, G.; Rizzardo, E.; Thang, S. H. *Polymer* **2008**, *49*, 1079–1131.
(32) Boyer, C.; Bulmus, V.; Davis, T. P.; Ladmiral, V.; Liu, J. Q.; Perrier, S. *Chem. Rev.* **2009**, *109*, 5402–5436.
(33) Zelikin, A. N. *ACS Nano* **2010**, *4*, 2494–2509.
(34) Chuang, H. F.; Smith, R. C.; Hammond, P. T. *Biomacromolecules* **2008**, *9*, 1660–1668.
(35) Smith, R. C.; Riollano, M.; Leung, A.; Hammond, P. T. *Angew. Chem., Int. Ed.* **2009**, *48*, 8974–8977.
(36) Vodouhe, C.; Le Guen, E.; Garza, J. M.; Francius, G.; Dejugnat, C.; Ogier, J.; Schaaf, P.; Voegel, J. C.; Lavalle, P. *Biomaterials* **2006**, *27*, 4149–4156.
(37) Schneider, A.; Vodouhe, C.; Richert, L.; Francius, G.; Le Guen, E.; Schaaf, P.; Voegel, J. C.; Frisch, B.; Picart, C. *Biomacromolecules* **2007**, *8*, 139–145.
(38) Zhang, X.; Sharma, K. K.; Boeglin, M.; Ogier, J.; Mainard, D.; Voegel, J. C.; Mely, Y.; Benkirane-Jessel, N. *Nano Lett.* **2008**, *8*, 2432–2436.